# A novel method for the synthesis of sub-microcrystalline wurtzite-type $In_xGa_{1-x}N$ powders

R. García [a],*, G.A. Hirata [b], M.H. Farías [b], J. McKittrick [c]

[a] *Programa de Posgrado en Física de Materiales CICESE-CCMC-UNAM, Km. 103 Carretera Tijuana-Ensenada, B.C., Mexico 22860, Mexico*
[b] *Centro de Ciencias de la Materia Condensada, Universidad Nacional Autónoma de México, A.P. 2681, Ensenada B.C., Mexico 22860, Mexico*
[c] *Department of Mechanical and Aerospace Engineering and Materials Science and Engineering Program, University of California at San Diego, La Jolla, CA 92093-0411, USA*

## Abstract

A novel method to synthesize wurtzite-type gallium–indium nitride powders ($In_xGa_{1-x}N$, $x = 0, 0.5, 1$) with small particle size, high purity and high crystallinity has been developed. The method produces finely divided powders via the pyrolysis reaction of a complex salt (ammonium hexafluoroindium-gallate, $(NH_4)_3In_xGa_{1-x}F_6$) in an ultrahigh purity ammonia flow inside of a quartz tubular reactor at relatively low temperature, 630 °C. The conditions of the process avoid the formation of metallic indium, oxides or fluorides. Scanning electron microscopy and X-ray diffraction analysis performed on these sub-micron particles of $In_xGa_{1-x}N$ show an hexagonal wurtzite-type structure, which is very similar to pure InN produced by the same technique. © 2002 Elsevier Science B.V. All rights reserved.

## 1. Introduction

High-efficiency light-emitting diodes emitting amber, green, blue, and ultraviolet light have been obtained through the use of an InGaN active layer instead of a GaN active layer [1]. The localized energy states caused by fluctuations of In composition in the InGaN active layer are related to the high efficiency of the InGaN-based emitting devices [1]. Light-emitting diodes (LEDs) based on these materials have been applied in flat-panel displays, and in blue and ultraviolet laser diodes. These laser diodes promise high-density optical data storage (Digital Versatile Disk, DVD) and high-resolution printing devices [2]. Also, blue LEDs are employed to pump integrated inorganic and organic media to produce colors reaching red, on one hand, and white light on the other. In addition to the traditional displays, these LEDs have applications in traffic lights, moving signs, indicator lights and, possibly, in light sources for accelerated photosynthesis and in medicine for diagnosis and treatment. Potentially, further improvement in LEDs would expand the applications to residential and commercial lighting with large energy savings as LEDs become more efficient than incandescent bulbs [3].

At present, there are several techniques to synthesize InGaN thin films such as Hydride Vapor Phase Epitaxy (HVPE), Metal Organic Vapor Phase Epitaxy (MOVPE) and Molecular Beam Epitaxy (MBE), which have yielded greatly improved film quality. Although there are numerous publications on the growth of InGaN films, there are no reports on the synthesis of InGaN powders.

In this work, a new method to produce wurtzite structure gallium–indium nitride ($In_xGa_{1-x}N$, $x = 0, 0.5, 1$) powders with small particle size, high purity and high crystallinity in the as-synthesized state is reported. This method is based in the technique that Juza and Hahn [4] utilized in 1940 to produce GaN and InN. However, some improvements have been made to avoid contamination of fluorine and to reduce the amount of oxygen in the solid solution. Several works

* Corresponding author.

[5–7] address the problem of metallic indium formation in the synthesis of $In_xGa_{1-x}N$ thin films. The new method reported in this work results in solid solution of $In_xGa_{1-x}N$ powders that avoids the formation of metallic indium by just controlling the time and temperature of reaction. The method produces finely divided powders and is carried out in three steps. First, gallium–indium hydroxide [$In_xGa_{1-x}(OH)_3$] is synthesized from the reaction of a stoichiometric solution of gallium nitrate [$Ga(NO_3)_3$] and indium nitrate [$In(NO_3)_3$] with ammonium hydroxide ($NH_4OH$), at room temperature. Then, the gallium–indium hydroxide is reacted with ammonium fluoride ($NH_4F$) at room temperature to produce a complex salt [$(NH_4)_3In_xGa_{1-x}F_6$]. Finally, this complex salt reacts with ammonia in a hot tubular furnace at 630 °C to produce sub-microcrystalline InGaN powders. The materials produced by this new method have were characterized by scanning electron microscopy (SEM), energy dispersive spectroscopy (EDS) and X-ray diffraction (XRD) techniques.

## 2. Experimental procedure

The procedure for the synthesis of $In_xGa_{1-x}N$ with $x = 0, 0.5, 1$ is illustrated in Fig. 1. The primary precursors were $In(NO_3)_3 \cdot H_2O$ (Puratronic, 99.999%),



Fig. 1. Flow diagram of the nitriding process by the pyrolysis reaction of a complex salt $(NH_4)_3In_xGa_{1-x}F_6$ in ammonia flow.

$Ga(NO_3)_3 \cdot 6H_2O$ (Puratronic, 99.999%) and ammonium hydroxide (25% $NH_3$, 99.99%). The required amount of each reactant was calculated from the desired mass of the products according to the following reaction:

$$x\,In(NO_3)_3(aq) + (1-x)Ga(NO_3)_3(aq)$$
$$+ 3NH_4OH(aq)$$
$$\Rightarrow In_xGa_{1-x}(OH)_3(s) + 3NH_4NO_3(aq). \qquad (1)$$
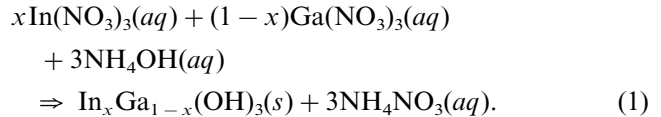
The nitrates were dissolved in a Pyrex beaker with deionized water. Then, the required amount of ammonium hydroxide was added, resulting in a viscous solution. The white solid compound (gallium–indium hydroxide) was separated through filtration. The white product was washed with deionized water until no change in the PH of water was registered. Then, the cleaned gallium–indium hydroxide was reacted with the ammonium fluoride concentrated solution in a Teflon beaker according to the following reaction:

$$In_xGa_{1-x}(OH)_3(s) + 6NH_4F(aq) \Rightarrow$$
$$(NH_4)_3In_xGa_{1-x}F_6(s) + 3H_2O(l) + 3NH_3(g). \qquad (2)$$
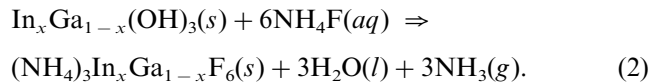
The Teflon beaker was introduced into a muffle furnace and heated at 200 °C for 12 h to dry the product (ammonium hexafluoroindium-gallate).

Once the ammonium hexafluoroindium-gallate was dry, it was placed in a tubular reactor (see Fig. 2) in a boron nitride crucible. The reactor consisted of a cylindrical quartz tube (5 cm in diameter and 80 cm length) with stainless steel flanges at both sides, which was introduced into a tubular furnace (40 cm length) with a maximum operating temperature of 1200 °C. Once the tubular reactor had been closed, an ultrahigh purity nitrogen flow (200 ml min$^{-1}$) was supplied through the inlet valve to remove the air from the reactor and to form an inert atmosphere. The center of reactor was heated until temperature reaches 1000 °C while the boron nitride crucible temperature was maintained at about 160 °C at the entrance of the reactor. Then, the inner part of the reactor was evacuated by a mechanical pump until reaching approximately 0.001 Torr. It was maintained under these conditions during 1 h in order to allow further drying of the ammonium hexafluoroindium-gallate and to reduce the oxygen contamination.

After 1 h, the temperature at the center of the reactor was lowered to about 640 °C, the $N_2$ flow was closed and, simultaneously, ammonia flow of 1000 sccm was introduced to the reaction chamber. Then, the crucible with the ammonium hexafluoroindium-gallate was placed at the center of reactor by using a magnetic manipulator (see Fig. 2). The reactor temperature was lowered about 10 °C and the following reaction was carried out:
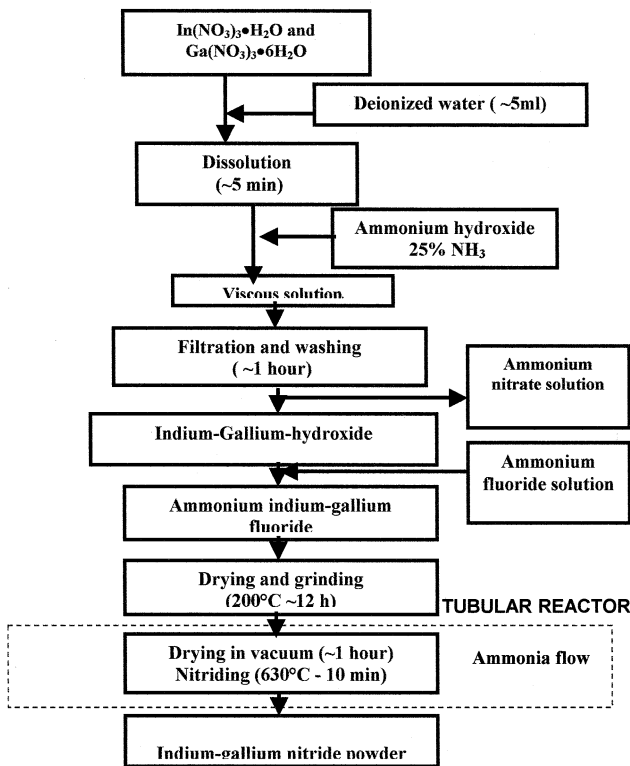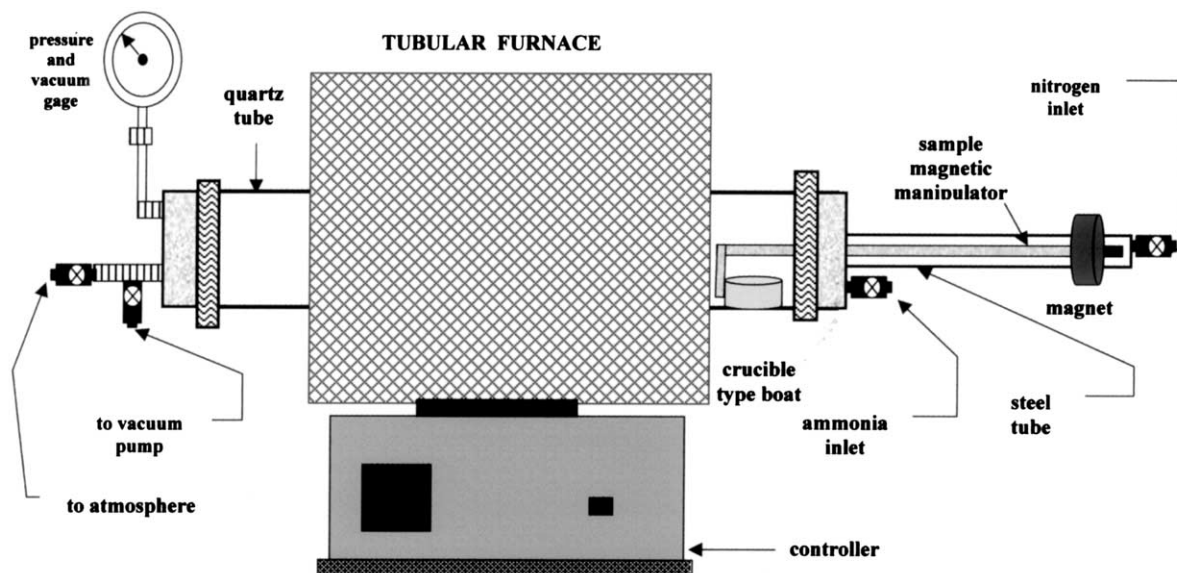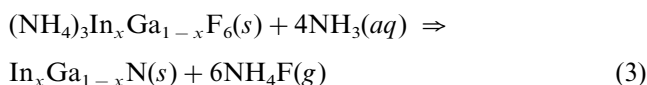
Fig. 2. A schematic representation of the tubular reactor.

$$(NH_4)_3In_xGa_{1-x}F_6(s) + 4NH_3(aq) \Rightarrow$$

$$In_xGa_{1-x}N(s) + 6NH_4F(g) \tag{3}$$

The reactor temperature was kept at 630 °C for 10 min and then lowered to 600 °C and held for another 25 min. Finally, the temperature was reduced to 520 °C for 20 min and then, using the sample magnetic manipulator, the crucible was pulled out to a cooler region (entrance) of the reactor.

The morphology of the powders was studied with a SEM operated at 10 kV. The elemental composition of the $In_xGa_{1-x}N$ powders was determined by EDS. Finally, XRD data were collected using a Philips diffractometer excited with $CuK_\alpha$ ($\lambda = 0.15406$ nm) radiation operated in the $2\theta$ mode. The lattice parameters ($a$ and $c$) were calculated by the relation: $\sin^2\theta = A(h^2 + hk + k^2) + Cl^2$, where $A = \lambda^2/3a^2$ and $C = \lambda^2/4c^2$ using the (100) and (002) peaks.

## 3. Results and discussion

A typical SEM image of the complex salt ammonium hexafluoroindium-gallate ($(NH_4)_3In_xGa_{1-x}F_6$) powder, which is the precursor of the $In_xGa_{1-x}N$, is shown in Fig. 3. The morphology of the particles are polyhedra presenting hexagonal and rectangular faces with a particle size between 10 and 50 μm.

SEM images of the GaN, $In_{0.5}Ga_{0.5}N$ and InN powder as-synthesized by pyrolysis of $(NH_4)_3In_xGa_{1-x}F_6$ in flowing $NH_3$ are shown in Fig. 4a, b and c, respectively. The morphology of the InN particles is hexagonal polyhedra not interpenetrated, and the particle-size distribution of the hexagonal polyhedron is between 1.5 and 4 μm. A schematic representation of an average

hexagonal polyhedron with real dimensions is shown in Fig. 5. The morphology of the GaN particles is a hexagonal polyhedron interpenetrated forming microspheres, and the particle-size distribution of the hexagonal polyhedra is between 0.6 and 1.5 μm. The morphology of the $In_{0.5}Ga_{0.5}N$ sub-micron particles is rounded hexagonal polyhedra with a particle-size distribution between 0.3 and 0.7 μm. The structure of this polyhedron (InGaN) is similar with the crystalline structure of the InN.

Fig. 6 a, b and c show EDS spectra for GaN, $In_{0.5}Ga_{0.7}N$ and InN, respectively. The main peaks are labeled and correspond to nitrogen (transition $K_\alpha$ at 0.392 keV), gallium (transitions: $L_\alpha^1$ at 1.096 keV and $L_\beta^1$ at 1.122 keV) and indium (transitions: $L\iota$ at 2.904
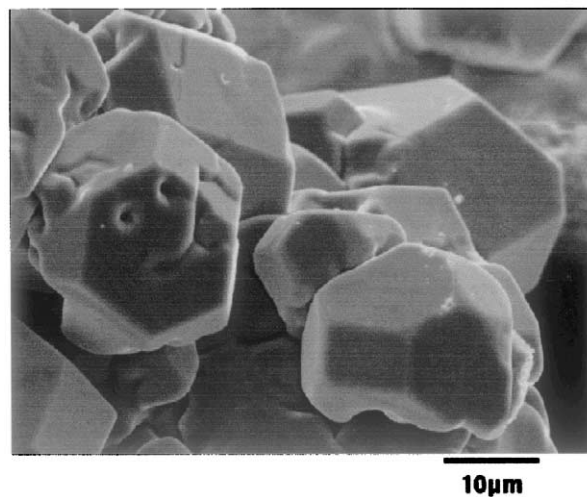


Fig. 3. SEM micrograph of ammonium hexafluoroindium-gallate ($(NH_4)_3In_xGa_{1-x}F_6$) powder, precursor of the $In_xGa_{1-x}N$.
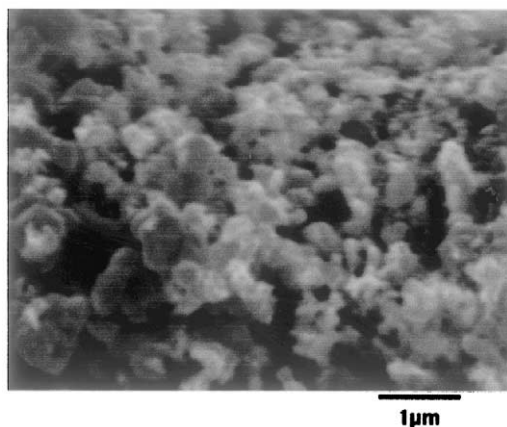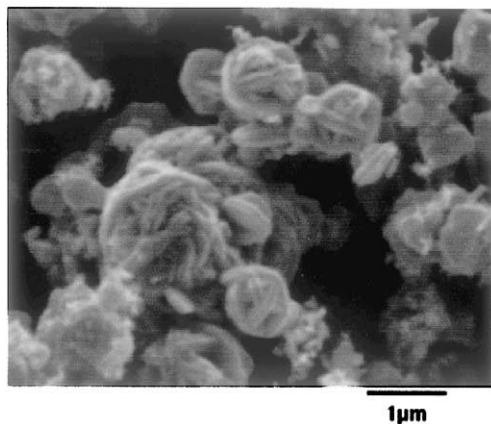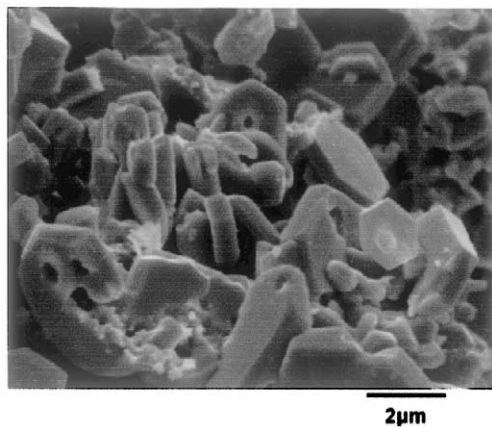
Fig. 4. (a) SEM micrograph of InN powders. Individual hexagonal submicron particles are observed; (b) SEM micrograph of GaN powders. Hexagonal particles are interpenetrated, forming microspheres; (c) SEM micrograph of $In_{0.5}Ga_{0.5}N$ powders. Rounded hexagonal particles are observed.

keV, $L_{\alpha}^{1}$ at 3.287 keV, $L_{\beta}^{1}$ at 3.487, $L_{\beta}^{2}$ at 3.713 keV and $L_{\gamma}^{1}$ at 3.920 keV). The fact that there are no other transitions, indicates the absence of impurities such as fluorine and oxygen, within the detection limits of the instrument. Relative atomic concentrations for In and Ga and subsequently the $x$ value in the $In_xGa_{1-x}N$ formula were obtained by considering sensitivity factors and EDS intensity measurements. Mixed powders of InN and GaN (prepared by the same method) with
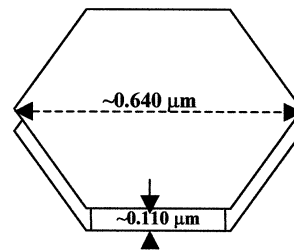


Fig. 5. Schematic representation of a typical hexagonal particle of GaN as observed from the SEM micrographs.
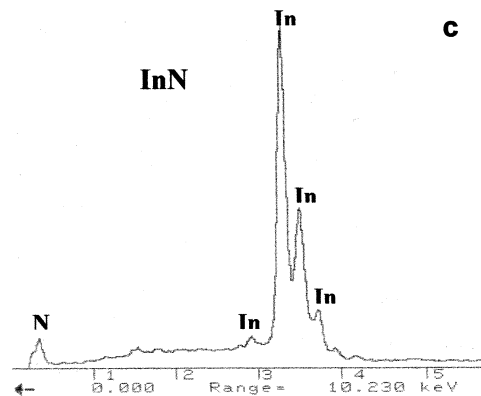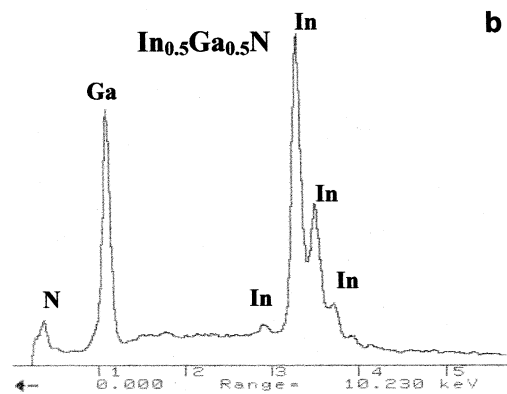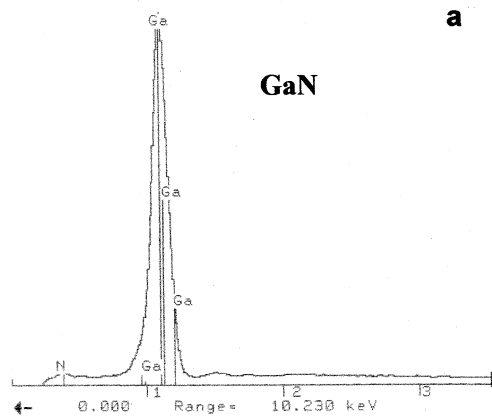


Fig. 6. EDS spectra for the: (a) GaN; (b) $In_{0.5}Ga_{0.5}N$; and (c) InN powders synthesized by the pyrolysis of a complex salt method.

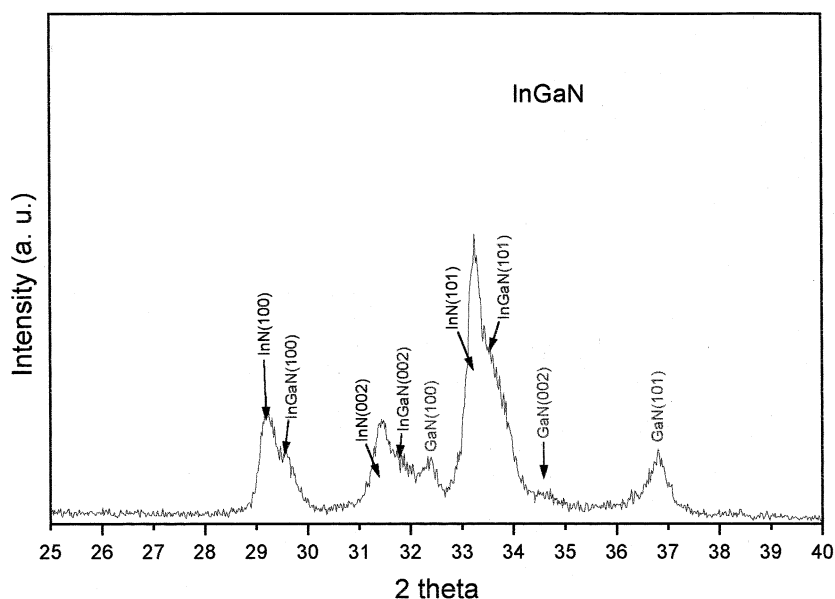Fig. 7. XRD spectrum of hexagonal (wurtzite type) $In_{0.5}Ga_{0.5}N$ powders synthesized by the pyrolysis method. Minor amounts of the crystalline phases GaN and InN are also present.

Table 1
Lattice parameters of GaN, $In_{0.5}Ga_{0.5}N$ and InN powders

| Parameter | GaN[a] | GaN[b] | InN[a] | InN[c] | $In_{0.5}Ga_{0.5}N^a$ |
| --- | --- | --- | --- | --- | --- |
| Crystal structure | Wurtzite | Wurtzite | Wurtzite | Wurtzite | Wurtzite |
| Lattice constant, $a$ (nm) | 0.3187 | 0.3186 | 0.3536 | 0.3536 | 0.3485 |
| Lattice constant, $c$ nm | 0.5185 | 0.5178 | 0.5700 | 0.5709 | 0.5488 |

[a] This work.
[b] JCPDS 02-1078.
[c] JCPDS 79-2498.

0.1, 0.2, 0.3, 0.4 and 0.5 mole fraction of InN, which were carefully weighted and fully mixed, were used as standard samples. The discrepancies of the $x$ value between the composition of the mixed powders and the composition determined from EDS measurement was less than 1% in all cases. Therefore, the accuracy in the relative atomic concentrations obtained by this method is considered to be of about 1%.

The XRD spectrum of the $In_{0.5}Ga_{0.5}N$ powder is presented in Fig. 7. This X-ray diffraction pattern shows a hexagonal (type wurtzite) crystalline structure with lattice parameters very similar to those of the InN. Small amounts of pure crystalline GaN, indexed from the JCPDS 02-1078 card, and InN, indexed from the JCPDS 79-2498 card, are indicated labeling the corresponding peaks in Fig. 7. There are no other cystalline phases present such as oxides, fluorides, or pure metals. Estimated lattice parameters of the GaN, InN and $In_{0.5}Ga_{0.5}N$ from experimental measurement are presented in Table 1. The lattice parameters of GaN and InN are in good agreement with those values reported by Edgar [8] for the hexagonal wurtzite structure as determined by the analytical method [9].

## 4. Conclusions

A new nitriding method for the bulk production of gallium−indium nitride powders ($In_xGa_{1-x}N$, $0 \le x \le 1$) with high purity, high crystallinity and sub-micron particle size is reported. Scanning electron microscopy images of the InGaN powders produced by the pyrolysis reaction method show particles with hexagonal morphology in the as-synthesized state with a particle-size distribution between 0.3 and 0.7 µm. Energy dispersive spectra show high purity in the nitrides produced by the pyrolysis of a complex salt method. Neither oxygen or fluorine are detected within the instrument accuracy. The results of X-ray diffraction of the $In_xGa_{1-x}N$ material show a hexagonal wurtzite structure very similar to the crystalline structure of InN. The lattice parameters of the InGaN fall between those of GaN and InN. The results indicate that the pyrolysis of the $(NH_4)_3In_xGa_{1-x}F_6$ in $NH_3$ atmosphere is excellent for the production of high purity, chemically homogeneous and well crystallized $In_xGa_{1-x}N$ powders in the as-synthesized state avoiding the formation of metallic indium

in the solid solution. Since these nitride compounds cannot be prepared by conventional methods, this method has significant importance for the synthesis of novel complex nitrides.

## Acknowledgements

## References

[1] S. Nakamura, Science 281 (1998) 956.
[2] F.A. Ponce, D.P. Bour, Nature 386 (1997) 351.
[3] H. Morkoc, Nitride Semiconductors and Devices, Springer-Verlag, Germany, 1999, p. 1.
[4] R. Juza, H. Hahn, Z. Anorg. Allg. Chem. 244 (1940) 111.
[5] S.M. Bedair, F.G. McIntosh, J.C. Roberts, E.L. Piner, K.S. Boutros, N.A. El-Masry, J. Crystal Growth 178 (1997) 32.
[6] R.A. Fischer, H. Sussek, A. Miehr, H. Pritzkow, E. Herdtweck, J. Organometallic Chem. 548 (1997) 73.
[7] H. Kanie, T. Kawano, K. Sugimoto, R. Kawai, Mat. Res. Soc. Symp. Proc. 621 (2000) Q5.11.1.
[8] J.H. Edgar, Properties of Group III Nitrides, INSPEC–IEE, London, UK, 1994, pp. 30–40.
[9] B.D. Cullity, Elements of X-Ray Diffraction, Addison-Wesley, USA, 1978, p. 324.